

Toxicology Research

Accepted Manuscript



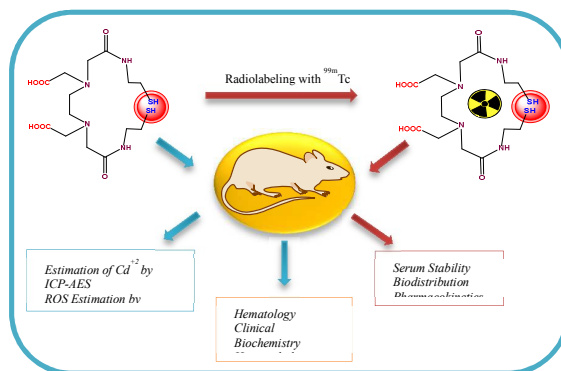
This is an *Accepted Manuscript*, which has been through the Royal Society of Chemistry peer review process and has been accepted for publication.

Accepted Manuscripts are published online shortly after acceptance, before technical editing, formatting and proof reading. Using this free service, authors can make their results available to the community, in citable form, before we publish the edited article. We will replace this *Accepted Manuscript* with the edited and formatted *Advance Article* as soon as it is available.

You can find more information about *Accepted Manuscripts* in the [Information for Authors](#).

Please note that technical editing may introduce minor changes to the text and/or graphics, which may alter content. The journal's standard [Terms & Conditions](#) and the [Ethical guidelines](#) still apply. In no event shall the Royal Society of Chemistry be held responsible for any errors or omissions in this *Accepted Manuscript* or any consequences arising from the use of any information it contains.

Graphical Abstract



Synthesis and in vivo toxicity assessment of radiolabeled Bis-ligand functionalized core shell
Quantum dots

ARTICLE

Synthesis and *in vivo* toxicity assessment of CdSe: ZnS Quantum Dots functionalized with EDTA-Bis- Cysteamine

Cite this: DOI: 10.1039/x0xx00000x

Received 00th January 2012,
Accepted 00th January 2012

DOI: 10.1039/x0xx00000x

www.rsc.org/

Narmada Bag^{a,b}, Rashi Mathur^{a*}, Firasat Hussain^b, Namita Indracanti^c, Sweta Singh^a, Shivani Singh^{a,b}, Ram Prakash Chauhan^d, Krishna Chuttani^a, Anil Kumar Mishra^{a*}

Abstract

The design and surface chemistry of the core shell quantum dots significantly affect their bio-distribution, kinetics and toxicity. Bis - ligand have shown to improve the loading capacity and control the steric ligand packing density on the quantum dot surfaces improving the biological properties and controlling the toxicity of the quantum dot nano-conjugates. In this study we have functionalized core shell CdSe:ZnS quantum dots with a homo-dimeric system (EDTA-Bis-Cysteamine) and evaluated their stability *in vivo* for diagnostic applications. This homo-dimeric N₂S₂ system wraps the quantum dots and has pendent carboxylate moieties for further conjugation chemistry. The novelty in the system is that it can be loaded with a variety of metal atoms through dative bonds even when the S atoms are attached to the ZnS shell. This results in formation of stable complex on a nano-platform for theranostic applications. The synthesized quantum dot nano-conjugate has been structurally evaluated using various analytical techniques. The spectrophotometric studies show emission of the nano-conjugate at 530 nm similar to the core shell. The haematology studies, biochemical assays and histopathology performed on the organs of interest showed no significant damage post injection over a time frame of 15 days. The generation of reactive oxygen species by cadmium based quantum dot nano-conjugate has been evaluated for the first time *in vivo* using Ferric Reducing Antioxidant Power assay (FRAP). The pharmacokinetics and bio-distribution of the nano-conjugate has been studied using radiolabelling (^{99m}Tc). After conjugation the blood kinetics show increased availability of the quantum dots in the blood pool and the bio-distribution pattern also shows major changes. However no significant toxic effects were observed during the time scale considered. This study highlights a facile route for designing small homo-dimeric ligand functionalized quantum dots nano-conjugates with favourable biological properties enhancing their potential to be used as multi-modal imaging/theranostic agents.

Introduction

Quantum dot (QD) have been a topic of intense research for their application as fluorescent and optical imaging agent in biology¹⁻³. It has been shown that both *in vitro* and *in vivo* the semiconducting quantum dots are useful in imaging and sensing.⁴⁻⁷ In spite of their evident advantages over the conventional organic dyes the application of these semiconducting quantum dots as *in vivo* imaging agent has been limited due to their inherent toxicity.⁸ This toxicity *in vivo* arises due to the (a) Release of toxic Cd²⁺ ion *in vivo* (b) Large surface-to-volume ratio which provides large surface for many oxidative, catalytic reaction and enzymatic reactions (c) Generation of

reactive oxygen species in response to quantum dots (d) Easy penetration inside the vital organs due to their ultra-small size which causes damage.⁹⁻¹⁷ Extensive research has been carried out for their modification which turns them into potential target specific optical imaging agent.¹⁸⁻¹⁹

It is therefore very important to understand this complex interplay of biological and cellular systems with the CdSe:ZnS core shell quantum dots for using them as *in vivo* optical imaging agent. *In vitro* toxicity of the quantum dots based on their size, shape, composition and design dependent intracellular localization has been extensively studied.¹⁶⁻²⁰ Bhatia et al have reported that CdSe core quantum dots are cytotoxic and induces cell death due to their inherent chemical composition, however

modifying their surface with ZnS and bovine serum albumin (BSA) significantly reduces the cytotoxicity, but does not completely eliminate it.¹⁶ One of the studies²¹ has also highlighted that quantum dot with amine-polyethyleneglycol coating and amphiphilic polymer coating were not cytotoxic in human keratinocyte (HaCaT) cells, while polyethleneimine coated quantum dots were highly toxic leading to increase in reactive oxygen species, decrease in mitochondrial membrane potential and DNA damage. These studies for sure indicate the importance of surface chemistry of these semiconducting quantum dots on their intracellular behavior and cytotoxicity. However in the in vivo conditions apparent discrepancies were observed as compared to the in vitro studies²²; this is understandable due to the dynamic nature of the in vivo system. As compared to the constant concentration exposure of quantum dots in vitro the in vivo system has all processes administration, distribution, metabolic reaction and excretion (ADME) happening simultaneously resulting in change in the available concentration of QD. This has led to lots of conflicting opinions on the applicability of quantum dot based system in vivo.

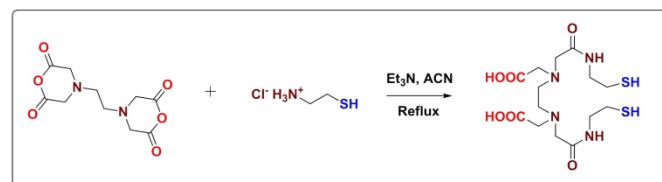
Recently some valuable information about the in vivo quantification assessment has been reported for the quantum dots with different size, shape, concentration, composition and chemical surface passivation. It has been found that the distribution and sequestration of these nanoparticles in organs does not induce any potential toxicity.²³⁻²⁷ In one of the earlier studies Tanya et al have reported the distribution, kinetics and in vivo toxicity of quantum dots synthesized using organometallic precursor. It was seen in the study that modification of the quantum dots with different surface chemistries showed no significant toxicity as observed in sprague dawley (SD) rats over a period of 80 days. Su et al have also shown that quantum dots synthesized in aqueous medium and passivated with small molecule like mercaptopropionic acid in vivo showed no significant toxicity 15-80 days post injection.²⁵ Further Tiwari et al have demonstrated the toxicity and in vivo behavior of anti-HER2 antibody conjugated CdSe/ZnS quantum dots in wistar rats. Their study suggests that the antibody coating assists in controlling any possible adverse effects of quantum dots. In all the above in vivo assessment no reproducible toxicity in physiologic doses was documented.²⁸

However, it is clear from both the in vivo and in vitro studies that the use of quantum dots depends on the tailoring of the surface chemistry which significantly affects the corresponding bio-distribution, kinetics and toxicity.²⁹⁻³² It has also been shown in one of our earlier studies that use of bis - ligands helps in making the hydrophobic quantum dots hydrophilic and at the same time it is responsible for controlling the ligand packing density of the quantum dots, an important parameter for optimizing emission intensity from the core. The conjugation of bio-vectors to this ligands also increased affinity and specificity toward the targets due to its ability to bind two binding sites simultaneously thereby improving target to non-target ratio.³³ Keeping this in mind here we have synthesized a homo-dimeric system (EDTA-Bis-Cysteamine). This ligand has N₂S₂ core which forms very stable tetradentate metal complexes with the Tc (V)³⁴ hence

conjugating the QD core with this ligand makes it convenient to study the pharmacokinetics of the QD nano-conjugate which is otherwise quite difficult to radiolabel due to the raw materials and synthetic procedures used. At the same time ^{99m}Tc can be replaced by other radiometals like ^{186,188}Re which is a β emitter and has similar chemistry with ^{99m}Tc. The rhenium complexes which are analogues of ^{99m}Tc have been used for therapy.^{35,36} In addition the ligand which is used here has many carboxylic groups which can be conjugated to therapeutic peptides and drugs using the amide conjugation making this system suitable for exploration in theranostics/ bimodal imaging.²⁷

The synthesized quantum dot nano-conjugate has been extensively evaluated using various analytical techniques. To demonstrate the biocompatibility we have evaluated all the blood parameters, liver and kidney functions by biochemical assays. As per the best of our knowledge we have in this paper for the first time used Ferric Reducibility Antioxidant Power assay (FRAP)^{37,38} in vivo to quantify the reactive oxygen species (ROS) generated in plasma and tissue of different organs arising due to the sequestration of the quantum dots. Histopathology of organs of interest help visualize the induced effect of quantum dots. Inductive coupled plasma atomic emission spectroscopy (ICP-AES) shows the cadmium ion concentration in various organs over a period of 15 days. Although ICP-AES is a well-known and efficient technique for metal ion estimation, it cannot confirm the state in which the metal ion is present i.e., in core shell nanocomposite or decomposed metallic form. Radiolabeling makes it easier to track and quantify ^{99m}Tc-EDTA-Bis-Cysteamine-QD as a whole over a short period of time (24 h). Hence both the radiolabeling and ICP-AES technique together give a better quantitative estimation of bio-distribution and pharmacokinetics of the QD nano-conjugate. The ^{99m}Tc-EDTA-Bis-Cysteamine-QD also contains many carboxylic groups on the surface which can be further conjugated to specific biomarkers for targeted imaging/ delivery.

Results and discussions



Scheme-1 synthesis of EDTA-Bis-Cysteamine

Synthesis of EDTA-Bis-Cysteamine ligand

The synthetic protocol used for the synthesis of the EDTA-Bis-Cysteamine ligand is shown in Scheme-1. The synthesis involves a facile one step procedure where the cysteamine hydrochloride reacts with EDTA anhydride at 70° C under reflux in presence of triethylamine in acetonitrile. The synthesis of the EDTA-Bis-Cysteamine ligand is confirmed by ¹H NMR, ¹³C NMR, and ESI-MS spectroscopy. In the ¹H NMR spectrum (Figure 1a) presence of triplet at 2.716 ppm, and 3.342 ppm confirms the EDTA-Bis-

Cysteamine conjugation. In the ^{13}C spectrum (Figure 1c) peaks at 168.98 ppm corresponds to the

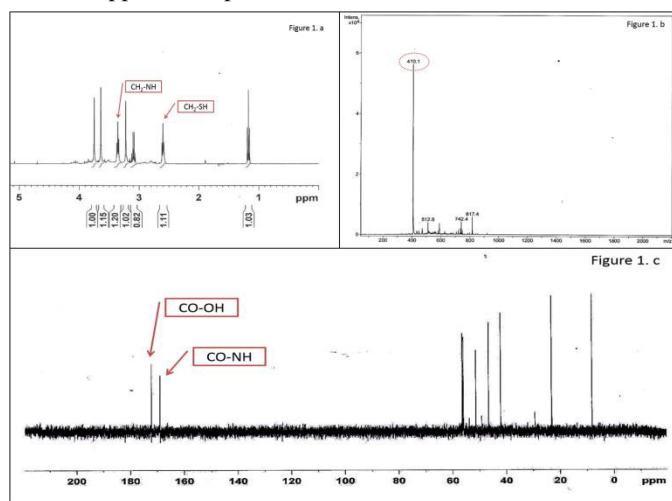


Fig. 1 Spectral analysis of EDTA-Bis-Cysteamine (a) ^1H NMR spectrum (b) ESI Mass Spectrum (c) ^{13}C NMR spectrum

newly formed amide carbonyl group while the peak at 172.20 ppm corresponds to the carboxylic carbonyl group. The m/z peak at 410 corresponds to the molecular ion peak shown in (Figure 1b).

Synthesis of EDTA-Bis-Cysteamine-QD Nano-Conjugate

The red light emitting CdSe/ZnS coreshell hydrophobic quantum dots were synthesized using a protocol reported earlier.⁴ The ligand exchange on the quantum dot surface was carried out in mixture of toluene and tetrahydrofuran (1:1) which was refluxed at 60°C for 2 h. The colour of the reaction mixture changes from brown to yellow which indicates the aqueous solubility of the nano-conjugate and also confirms the surface passivation of the quantum dot with EDTA-Bis-Cysteamine. The EDTA-Bis-Cysteamine-QD nano-conjugate

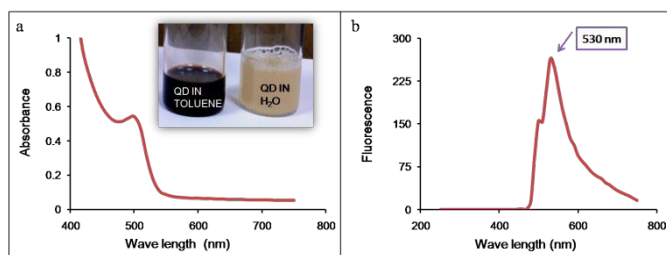


Fig. 2 UV-VIS and Fluorescence spectra of EDTA-Bis-Cysteamine-QD nano-conjugate (a) excitation at 500 nm (b) emission at 530 nm

synthesis is evaluated spectrophotometrically and by transmission electron microscopy. The nano-conjugate shows an absorbance at 500 nm (Figure 2a) and emission at 530 nm (Figure 2b). The quantum dot nano-conjugate maintains its optical properties after surface modification and the quantum yield of the aqueous solubilized nano-conjugate is 40% with a FWHM of 60-70 nm.

The size of the nano-conjugate was found to be 7-9 nm as measured by TEM (Figure 3).

EDTA-Bis-Cysteamine conjugated quantum dots are stable in aqueous medium for months at 40°C without any precipitation. The attachment of quantum dots to EDTA-Bis-Cysteamine provides carboxylic groups on the surface which can be further used for conjugation of biomolecules to make the quantum dots target specific. The structure of the EDTA-Bis-Cysteamine-QD nano-conjugate as shown in the Scheme 1 shows a cavity like structure which is available for the efficient binding of $^{99\text{m}}\text{Tc}$. The well-defined binding of the $^{99\text{m}}\text{Tc}$ enable us to evaluate the bio-distribution and pharmacokinetics of the nano-conjugate in vivo.

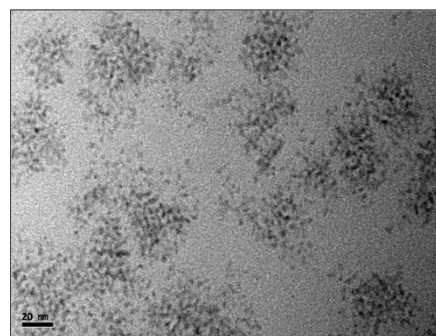


Fig. 3 TEM image of QD-EDTA-Bis-Cysteamine nano-conjugate

Serum Stability, Blood Kinetics and Biodistribution

Both the EDTA-Bis-Cysteamine molecule and EDTA-Bis-Cysteamine-QD nano-conjugate were radiolabeled with $^{99\text{m}}\text{Tc}$. To achieve the maximum labelling efficiency all the labelling parameters such as temperature, pH, concentration of the reducing agents (SnCl_2) were standardized. The proteolytic degradation of the radiolabelled quantum dot nano-conjugate was determined in serum in vitro. ITLC analysis revealed that the $^{99\text{m}}\text{Tc}$ -EDTA-Bis-Cysteamine molecule and $^{99\text{m}}\text{Tc}$ -EDTA-Bis-Cysteamine-QD nano-conjugate remained sufficiently stable during incubation at 37°C with serum. A maximum of 5-6% of radioactivity degraded after 24 h of incubation advocating a high in vitro stability (90-95%) of $^{99\text{m}}\text{Tc}$ -EDTA-Bis-Cysteamine-QD up to 24 h (Figure 4).

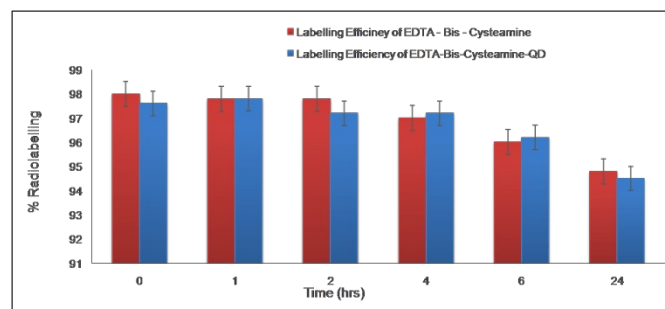


Fig. 4 Radiolabelling efficiency and serum stability studies of $^{99\text{m}}\text{Tc}$ -EDTA-Bis-Cysteamine and $^{99\text{m}}\text{Tc}$ -EDTA-Bis-Cysteamine-QD nano-conjugate

According to the blood kinetics data the blood clearance of ^{99m}Tc -EDTA-Bis-Cysteamine-QD is slow as compared to the ^{99m}Tc -EDTA-Bis-Cysteamine molecule which indicates higher availability in blood circulation and hence has higher possibility of reaching the target site. This implies that after conjugation of biomolecules a better contrast can be expected for diagnostic imaging.

The bio-distribution of ^{99m}Tc -EDTA-Bis-Cysteamine-QD and ^{99m}Tc -EDTA-Bis-Cysteamine showed very interesting results. The bio-distribution of ^{99m}Tc -EDTA-Bis-Cysteamine shows maximum accumulation in kidney ($10.11 \pm 1.13\%$ injected dose/gram (ID/gm) one hour post-injection, which remains at ($5.94 \pm 1.17\%$ ID/gm) after 24 h. while the maximum uptake in all other organs over the 24 h period remains below 2% ID/gm. This indicates that the molecule shows renal clearance (Figure 5).

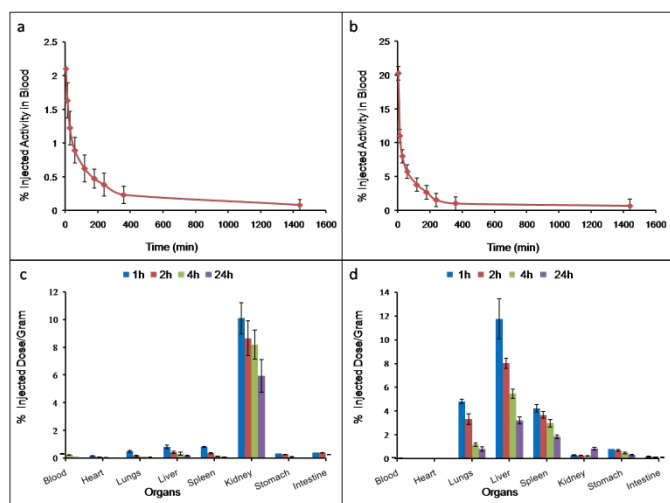


Fig. 5 Blood kinetics and bio-distribution pattern of (a) (c) ^{99m}Tc -EDTA-Bis-Cysteamine (b)(d) ^{99m}Tc -EDTA-Bis-Cysteamine-QD nano-conjugate respectively.

However after the quantum dot was conjugated to ^{99m}Tc -EDTA-Bis-Cysteamine, the nano-conjugate shows drastic change in bio-distribution pattern. High accumulation is seen in liver ($11.76 \pm 1.18\%$ ID/gm), lungs ($4.8 \pm 0.89\%$ ID/gm) and in spleen ($4.23 \pm 0.32\%$ ID/gm) one hour post injection. While in all other organs the accumulation is less than 2% ID/gm over the 24 h of period including kidney. The biodistribution of bis molecule changes completely on attaching with the quantum dots as the maximum uptake is seen in the RES system i.e., liver, spleen and lungs due to the large number of macrophage cells.³² This might also be attributed to the fact that the ligand which is an organic molecule follows a charge dependent clearance via the kidney however as soon as the QD is attached the clearance is governed by the size dependent property. As the size becomes greater than the 5 nm threshold the renal excretion of the QD nanoconjugate is restricted.³⁹

The drastic change seen in bio-distribution pattern prompted us to do the ICP-AES for liver, kidney and spleen (Figure 6). The liver shows a very high accumulation of Cd^{+2} ion $34.12 \pm 1.1\%$ ID/gm 24 h post injection as could also be seen in the biodistribution studies. Fischer et al have also shown that

intracellular sequestration of quantum dots in such percentage show no phagocytic impairment.⁴⁰

Interestingly it is observed that the low percentage of cadmium in kidney which is seen after 24 hrs goes up over a period of time from 6% ID/gm at day 3 to 34 %ID/gm on day 15 respectively. A significant increase in accumulation was also observed in spleen. It is possible that the quantum dot nano-composite which is approximately 6-9 nm in size initially accumulates in liver. Overtime the QD nanoconjugate is metabolised in the liver into biologically benign compounds which are then eliminate through the normal renal clearance. However some of the QD nanoconjugate may have decomposed to metallic cadmium ion due to the presence of hypochlorous acid in phagocytic cells followed by sequestration of cadmium ion by kidney leading to increased concentration over 15 days. However both the ICP-AES and biodistribution studies are in close agreement on

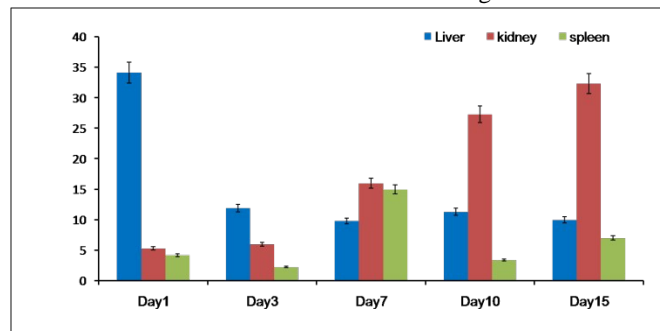


Fig. 6 ICP-AES showing Cd^{+2} concentration in liver, kidney and spleen 15 days of post-injection

the distribution pattern as well as the intactness of the nano-conjugate as there is no uptake in the kidney 24 h post injection.

Scintigraphy

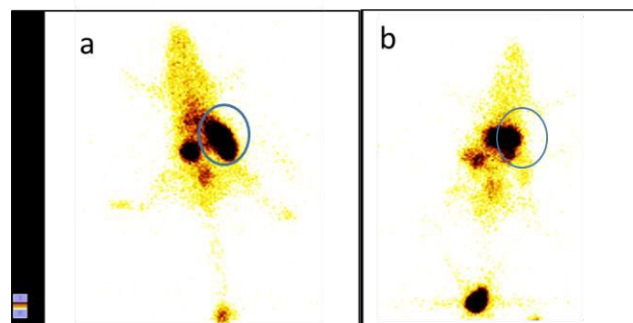


Fig. 7 Scintigraphic image of (a) ^{99m}Tc -EDTA-Bis-Cysteamine (b) ^{99m}Tc -EDTA-Bis-Cysteamine-QD nano-conjugate respectively 4 hrs post injection.

The biodistribution is supported by the scintigraphic image recorded 4 h post injection. In Fig. 7a. we observe that ^{99m}Tc -EDTA-Bis-Cysteamine shows fast clearance and accumulation only in kidney. On the other hand the ^{99m}Tc -EDTA-Bis-Cysteamine-QD (Fig. 7 b.) nano-conjugate shows a completely different distribution pattern. We observed low accumulation in kidney while a substantial distribution

of the radiolabeled nano-conjugate was found in liver and spleen. This can be attributed to the opsonisation effect, a major *in vivo* phenomena which is observed on use of nanoparticles and at the same time it is also the behaviour cadmium based quantum dots show *in vivo*. As can be seen through the scintigraphic images the small molecule (EDTA-Bis Cysteamine) shows a very fast wash out through the renal route in the bargain showing maximum accumulation in the kidney however as soon as the quantum dots are conjugated to it the route of clearance or rather the distribution pattern changes significantly. This highlights in addition to understanding the change in biodistribution due to quantum dots in this QD nanoconjugate also shows a potential for use as agent for SPECT imaging hencing making it eligible as a bimodal imaging agent.

Quantification of ROS Generation by FRAP Assay

The leaching out of the toxic cadmium ion *in vivo* results in generation of reactive oxygen species (ROS) and subsequent oxidative stress induced tissue damage. *In vitro* assessment of the ROS generation has been extensively studied.^{41, 42} FRAP has been used for studying the antioxidant property of non-enzymatic defenses in biological fluids to understand the ability to resist oxidative damage. This method has been identified as one of the most efficient method (Benzie and Strain) for the evaluation of the antioxidant capability. We have used this assay here to our advantage for studying the *in vivo* ROS generation by QD based nano-conjugate in plasma and various tissue homogenates.

This study was performed in plasma over a period of 15 days. Blood samples were collected on day 1, 3, 5, 7, 15 respectively. A decrease in Fe⁺² concentrations was observed in plasma of treated animals as compared to the control value 24 h post injection. This is probably due to the fact that the non-enzymatic antioxidants present in the plasma are insufficient to scavenge the total amount of ROS generated, due to the long circulation time of the QD nano-conjugate in plasma hence activating immunosuppression. However 15 days post injection the concentration of Fe⁺² in plasma becomes equivalent to the Fe⁺² value in control indicating the restoration of the antioxidant level and defence mechanism (Figure 8a & 8b).

In case of the tissue homogenates increase in the concentration of Fe⁺²/gram tissue weight is observed as compared to control values. This is probably due to the synergistic scavenging of the generated ROS both by the enzymatic and the non-enzymatic antioxidant present in the tissue homogenates of the organs of interest.

The FRAP assay of the tissue homogenates also supplements our observations in the bio-distribution studies. The 24 h FRAP assay on the organs of interest show significant increase in Fe⁺² concentration in liver, spleen and lungs as compared to control as is seen in Table 1. Liver shows an almost double of the Fe⁺² concentration as compared to the control. This has also been observed in bio-distribution where at 24 h maximum uptake of the QD nano-conjugate is seen in the liver *in vivo* and highest percentage of Cd⁺² ion is observed by ICP-AES. However in kidney the Fe⁺² concentration is almost the same as the control thereby confirming no uptake of the QD nano-conjugate in

kidney 24h post injection. As FRAP assay values for plasma returned to control values within 15 days we did not extend the period of our study.

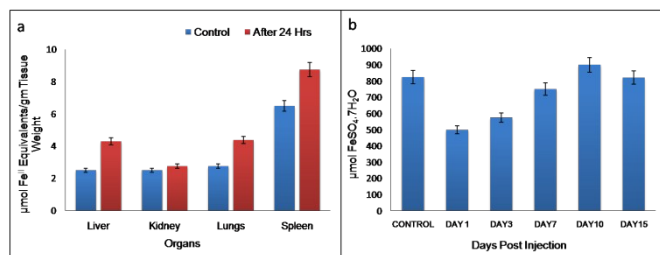


Fig. 8 (a) FRAP assay showing the Fe⁺² concentration in plasma at different time interval of post injection (b) in tissues of liver, spleen and kidney 24 hrs of post injection

Table 1 Quantitative estimation of Fe⁺² concentration in tissue homogenates of control and treated 24 hrs of post injection.

Tissue homogenates	Control*	Treated#
Liver	2.5±0.5 µmol	4.3±.01 µmol
Spleen	2.75±.01 µmol	4.37±.02 µmol
Lungs	6.5±.03 µmol	8.75±.07 µmol

*Control: Rat injected with saline. #Treated: Rat injected with EDTA-Bis-Cysteamine-QD

Hematology

The first interaction of an intravenously injected quantum dot nano-conjugate is with blood and its component. Therefore changes in the hematologic parameters are representative of the increase/ decrease of the activity of the immune system. In the haematology study it has been found that there is no change in the red blood cells count and red blood cell indices (mean corpuscular volume, mean concentration hemoglobin, mean concentration hematocrit, and red cell distribution width), hemoglobin and hematocrit over 15 days post injection Table 2. The samples were collected 1, 3, 5, 7, 15 days post injection respectively. There is no change in the platelet count. However a significant decrease in white blood cells count has been observed 24 h post injection. This may be due to many factors therefore we did the measurement of the WBC differentials (granulocytes, lymphocytes). No significant alteration in the WBC differentials is observed. This indicates that the change in WBC counts is due to the response of the immune system to the nano-conjugates in blood. The initial decrease however increases over 3-10 days reaching control values after 15 days.

Clinical Biochemistry

According to the studies done the major organs for the accumulation of quantum dot nanoconjugate over time have been either liver or kidney. Therefore to evaluate the liver and kidney functions biochemical assays like aspartate aminotransferase (AST), alanine aminotransferase (ALT), total bilirubin and creatinine have been carried out respectively (Figure 9). The AST and ALT are generally distributed in the liver and a rise in

ARTICLE

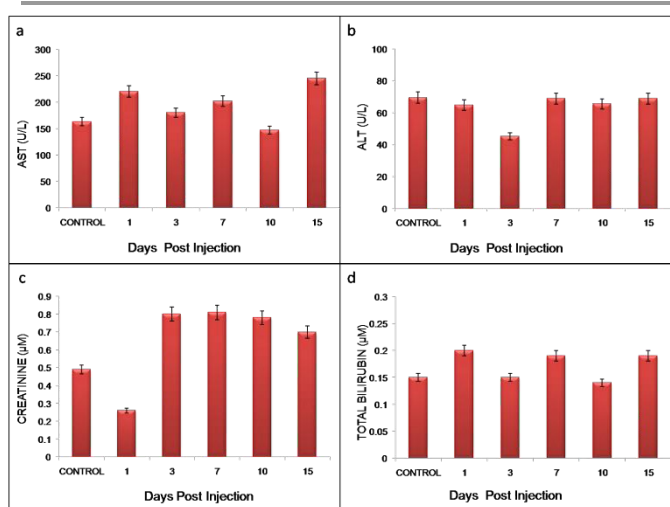
their value indicates necrosis in the liver cells. In our experiment a moderate elevation in AST level (less than two times) has been observed. However as the AST is also found in the cardiac/skeletal muscles we performed the more liver specific ALT.

The ratio of AST and ALT is found to be greater than one and the total bilirubin level is also not significantly altered over the 15 days of post injection. This clearly shows no liver injury as the ratio of AST/ALT of less than 1 indicates liver injury.

All the above discussed parameters ruled out the possibility of liver damage. Kidney function was evaluated by checking the creatinine level and the values are found within the acceptable range. (0.2- 0.9 mg/dl)

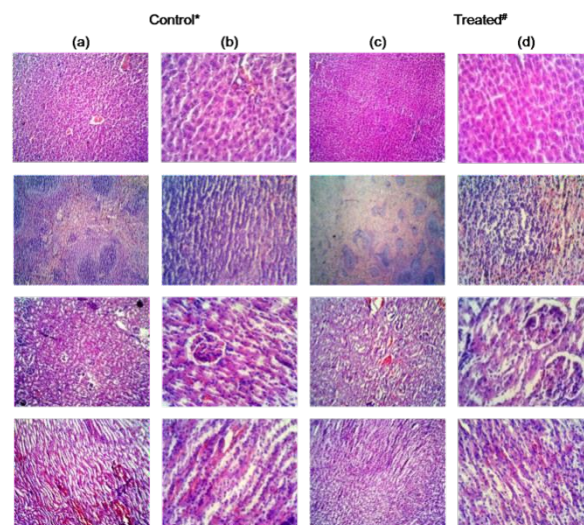
Both the hematological and biochemical analysis concludes that no major toxicity was observed after 15 days of post injection. Further the results are also confirmed by correlating the histopathology of respective organs.

Fig. 9 Clinical biochemical analysis (a) AST (aspartate aminotransferase) (b) ALT (alanine aminotransferase) (c) creatinine (d) total bilirubin content at different interval of injections.



Histopathology

Histopathology of the organs of interest viz., liver, kidney and spleen was carried out 15 days post injection to visualize any macroscopic changes indicating toxicity (Figure 10). At 10x magnification the morphology of tissue of spleen, liver, and kidney are seen to be normal as compared to control. In the liver tissue distribution of hepatic cells are normal, central vein, portal triad and nucleus with distinct cell membrane are clearly visible. Apart from some kupffer cell activation and mild degree of inflammatory cells around the portal area no significant damage was found in liver. In kidney also tissue morphology is well defined in both the outer cortex and inner medulla region. Glomerulus is clearly visible with distinct corpuscular space. Although in some region mild tubular degeneration, necrosis, pyknosis and cytoplasmic vacuolation has been seen, this does not refer to any kind of severe kidney damage. In the tissues of spleen the tissue morphology is well defined in both control and treated group. The red pulp and white pulp region are well



*Control: Rats Injected With Saline; #Treated: Rats Injected with EDTA-Bis-Cysteamine-QD

distributed and RBC breakdown products are clearly visible in both the control and treated group. In some areas mild defused degeneration of white pulp has been encountered. All the above microscopic pathological changes however do not indicate any severe tissue damages.

Fig. 10 . Hematoxylin and Eosin stained tissue photomicrograph of control and treated SD rat 15 days post injection magnification 10x (a) Liver, spleen, kidney (cortex and medulla) of control (b) Liver, spleen, kidney (cortex and medulla) of treated rats. Magnification 40x (c) Liver, spleen, kidney (cortex and medulla) of control (d) Liver, spleen, kidney (cortex and medulla)

Evidence of biocompatibility of the nano-conjugate over 15 days

It is well known that the cadmium based quantum dot nanoconjugates target the liver, spleen and kidney, this is also seen in the bio-distribution studies 24 hrs post injection. After 24 hrs from the ICP- AES studies it was seen that the cadmium content show increase in the kidney (3.850 ppm/gm tissue), and decrease in the liver (0.435 ppm/gm tissue) which indicates the degradation of the conjugate and release of the Cd⁺² ions. The release of Cd⁺² and their accumulation in the kidney was evaluated to understand if there was any toxicity with time due to the generation of ROS in kidney. The ROS if generated would result in histology changes in the kidney. We therefore performed histopathology on the organ of interest i.e., kidney of the treated animals and compared the tissue images with the control animal. No major histopathological alteration are encountered both in the medulla or the cortex region of the kidney. In addition to this the biochemical assays which were performed on the kidney and liver also showed that their values became comparable to that of the control animals. Two treated SD rats went continuous evaluation for a period of one month and showed no ill effects. This confirmed our assumption that the cadmium ions which are released at the concentrations used do not cause any severe damage in the timescale considered even if they are retained in vivo. However a study can be done to study the long term effects.

CONCLUSION

The current studies show that EDTA-Bis-Cysteamine conjugated cadmium based quantum dots shows no acute toxicity in the time scale considered. Most of the haematology and biochemical markers are in the normal range except mild variations in the WBC which indicate an expected response of the immune system to the quantum dot nano-conjugate. However since we are focussing on diagnostic imaging and as most of the physiological parameters come back to control values in 15 days time this molecule shows good potential. Also the attachment of a stable ligand on the surface of the core-shell quantum dot provides opportunity for designing target specific agents. The study also highlights that such small bis molecules based QD nanoconjugates can provide a good platform for tailoring nanoconjugates with optimized ligand packing density, optical property and controlled pharmacokinetics for favourable biological properties.

Experimental

Synthesis of EDTA-Bis-Cysteamine: Initially EDTA anhydride (3.90 mM) was dissolved in 10 ml of acetonitrile (ACN) in a three neck round bottom flask (50 ml) and refluxed at 70°C under nitrogen till the turbid solution becomes clear. To the above reaction mixture cysteamine hydrochloride (7.81mM) and triethylamine (7.81mM) was added simultaneously and refluxed for 72 h. After completion of the reaction the solution was evaporated to dryness and repeatedly washed with dichloromethane (DCM) to remove triethylamine. The final compound was sticky and yellow in colour. ¹H NMR (D₂O, 400MHz), 3.206 (t, CH₂-N), 3.374 (s, CH₂-NH-CO), 2.617 (t, CH₂-SH), 3.848 (s, CH₂-CO-NH), 3.607 (s, CH₂-COOH), 1.154 (t, CH₂, (CH₃CH₂)₃N), 3.129 (q, CH₃, (CH₃CH₂)₃N). ¹³C NMR (D₂O, 400MHz); δ (ppm); 56.45 (CH₂-COOH), 56.07 (CH₂-CONH), 53.86 (CH₂-N), 42.15 (CH₂-NH-CO), 29.43 (CH₂-SH), 168.98 (CO-NH), 172.20 (COOH), 46.62 (CH₂, (CH₃CH₂)₃N), 8.19 (CH₃, (CH₃CH₂)₃N). m/z (ESI) calculated for C₁₄H₂₆N₄O₆S₂ 410.13, found 410.1. The calculated value for elemental analysis was C = 40.96%, H = 6.38%, N = 13.65%, O = 23.38%, S = 15.62 and the observed values are C = 41.56%, H = 7.13%, N = 13.05%, O = 23.98%, S = 16.22%.

Synthesis of QD-EDTA-Bis-Cysteamine: The CdSe/ZnS core shell quantum dots with emission wavelength at 530 nm were synthesized using protocol described earlier are dissolved in toluene in a round bottom flask. To the above solution EDTA-Bis-Cysteamine in a mixture of water and tetrahydrofuran (1:1) was added and kept for reflux at 60°C for 2 h. Initially the colour of the reaction mixture was brown and as soon as the phase transfer of quantum dots takes place from toluene to water it changes to light yellow. The aqueous phase transfer and the colour change confirm the attachment of the EDTA-Bis-Cysteamine ligand over the quantum dot surface. The reaction mixture after keeping for few minutes at room temperature shows precipitate formation. Then the solution was centrifuged

to collect the EDTA-Bis-Cysteamine conjugated quantum dots and dissolved in phosphate buffer saline (PBS) for further use.

Physicochemical Characterization: The synthesis of the EDTA-Bis-Cysteamine ligand was characterized by ¹H NMR, ¹³C NMR and mass spectroscopy. The absorbance and emission wavelength of the synthesized EDTA-Bis-Cysteamine-QD nano-conjugate was recorded in a spectrophotometer. The size of this nano-conjugate was measured by transmission electron microscopy (TEM).

In Vitro Serum Stability: The metabolic stability of the EDTA-Bis-Cysteamine and EDTA-Bis-Cysteamine-QD was ascertained in vitro in collected serum samples. Serum was prepared by allowing blood collected from animals to clot for 1 h at 37°C in a humidified incubator maintained at 5% carbon dioxide and 95% air. The samples were then centrifuged at 400 g and the serum was filtered through a 0.22 μm filter into sterile plastic culture tubes. 100 mL of ^{99m}Tc labelled formulation was incubated respectively in 900 μL of this serum (in duplicate) at 37°C and analyzed to check for any dissociation by Instant thin layer chromatography (ITLC) using silica gel strips and 0.9% NaCl aqueous solution (saline) as a developing solvent. The change in labelling efficiency was monitored over a period of 24 h.

Animal Handling and Preparation for In Vivo Studies: All animal experiments and study protocols were approved by the Committee for the Purpose of Control and Supervision of Experiments on Animals (CPCSEA), Government of India, New Delhi. Animal handling and experimentation were carried out as per the guidelines of the Institutional Animal Ethics Committee. Male spargue-dawley (SD) rats of age 6-8 weeks are given food and water ad libitum and housed in a 12h/12 h light and dark cycle.

In Vivo Biochemical Studies: 6 sets of animals (each set n=5) were prepared for biochemistry, haematology, FRAP, ICP-AES, and histopathology studies. The animals were sacrificed at 1, 3, 7, 10 and 15 days post injection respectively. At the beginning of the experiment the control set (n=5) was injected with physiological saline while the 5 experimental set animals were injected with 200 μL of 15 nM EDTA-Bis-Cysteamine-QD solution. The blood sample was collected immediately after cardiac puncture and stored in anticoagulant vials for blood and plasma studies. The representative organs were harvested at the same time after the animal was sacrificed.

Radiolabeling: An aqueous solution of EDTA-Bis-Cysteamine-QD (9.78 nM) was taken in a shielded vial and stannous chloride was added. The pH of the resulting solution was adjusted to 6.5–7.0 with 0.5 M NaHCO₃. Then the mixture was passed through a 0.22 μm Millipore filter into a sterile vial. Freshly eluted ^{99m}TcO₄⁻ (93.7 MBq) was added and the complex was incubated for 30 min at room temperature for optimum labelling yield. The labelling efficiency was estimated using ITLC-SG as the stationary phase and 100% acetone as the mobile phase. The paper chromatography demonstrated the absence of unbound Na^{99m}TcO₄.

Blood Kinetics and Bio-Distribution: Blood clearance of ^{99m}Tc-labeled nano-conjugates was studied in healthy SD rats (n

ARTICLE

= 3) 100 μ Ci of the radiolabeled complex in saline was administered intravenously through the tail vein of the rats. Blood samples were collected using the retro orbital procedure. The Blood was collected from this area in anesthetized rats using a micro-hematocrit tube at different time intervals ranging from 5 min to 24 h. Persistence of activity in the circulation was calculated as percentage injected dose per whole blood, assuming a total blood volume as 7% of the body weight. The radioactivity of the precipitate and supernatant was measured using a well-type gamma spectrometer.

The SD rats were administered 100 μ Ci of 99m Tc labelled nano-conjugate, respectively, through the tail vein (IV). At 1, 2, 4 and 24 h post injection, the animals (n = 3) were euthanized and blood was collected by cardiac puncture into pre-weighed tubes. The rats were then dissected and different organs (heart, lungs, liver, spleen, kidneys, stomach, intestine, muscle) were removed, weighed and their radioactive counts were taken with the help of a gamma counter. Uptake of the radiolabeled compound into each organ was measured per gram of the tissue/organ and expressed as the percentage injected dose per gram (% ID/gm) organ weight. The radioactivity remaining in the tail (point of injection) was also measured and taken into account while calculating the radioactivity.

Scintigraphy

100 μ L of 99m Tc labelled –EDTA-Bis-Cysteamine and 99m Tc labelled EDTA-Bis-Cysteamine-QD were injected in SD rats and images were taken 4 h post injection i.e., time of maximum uptake.

Determination of Cadmium Ion by ICP-AES: The ICP-AES studies were performed for the calculation of Cd⁺² ion concentration at different time interval in selective representative organs. The representative tissue sample of liver, kidney and spleen were collected on day 1, 3, 7, 10 and 15 post injection. The collected tissues were washed, weighed, homogenized and digested with 70% nitric acid. The digested samples were diluted with double de-ionized water to 10 ml. The total concentration of Cd⁺² ions in the organ is calculated by the following formula.²⁵

$$\%ID/gm = QDTS \times VTS / QDIS \times VIQD \times WWT$$

Where, QDTS = QD in tissue, VTS = Volume of tissue sample, QDIS = QD in injected sample, WWT = Wet weight of tissues

Reactive oxygen species estimation in plasma and tissue by FRAP assay: The reactive oxygen species generation or the antioxidant capacity determination is done by FRAP assay. For the study organs (liver, kidney, and spleen) are removed 24 h post injection and immediately immersed in chilled Kill (1.15%) 10% w/v solution and then homogenized and centrifuged respectively. The FRAP assay was then carried out with the tissue homogenate and their reducing ability to resist oxidative damage was estimated. To check the reducing ability of the plasma, blood sample after 1, 3, 7, 10, 15 days of post injection was collected with 20 mg/ml EDTA anticoagulant. Of this sample, blood plasma was collected and used for FRAP analysis.

Haematology and Biochemical Analysis: Biochemical markers specific for liver (alanine aminotransferase (ALT), aspartate aminotransferase(AST) and kidney function (creatinine and bilirubin) are measured in a semi-automatic biochemistry

analyzer (RANDOX, RXmonza, UK) The assays are performed on these organs as maximum accumulation of the nano-conjugate has been found in them as per bio-distribution. For the quantification of the in vivo toxicity all the blood parameters like red blood cells RBC, white blood cells WBC, platelets count (PLT), mean corpuscular volume (MCV), mean corpuscular concentration (MCHC), hemoglobin (HGB), hematocrit (HCT), and all the differential parameters are also measured by haematology analysis in veterinary haematology analyzer (NIHIN KOHDEN, MEK-6450K,Celtac α , Japan). For these studies animals are euthanized and blood samples are collected from the rats by cardiac puncture 1, 3, 7, 10, 15 day post injection of quantum dots nano-conjugate. The animals are then sacrificed.

Histopathology: For histopathology studies the animals are sacrificed after 15 days post injection and selected organs (liver, kidney, spleen) were collected washed with saline and fixed with 10% buffered formalin for 48 h. After being processed in series of alcohol and xylene the tissues were embedded in paraffin wax and their 5 μ m thick sections are cut using semiautomatic tissue processor (spencer's tissue processor unit) followed by staining with hemotoxylin and eosin. It is then examined under light microscope for evaluation of histopathological changes.

ACKNOWLEDGEMENTS

The authors would like to thank Director INMAS, for his constant support and encouragement in carrying out this work. We are also thankful to Delhi University, India for providing characterization facilities. One of the authors is thankful to University Grants Commission, for the financial support.

^a*Department of Cyclotron and Radiopharmaceutical Sciences, Institute of Nuclear Medicine and Allied Sciences, Defence Research and Development Organization, Brig. S.K. Mazumdar Marg, New Delhi-110054, India*

^b*Department of Chemistry, Delhi University, New Delhi-110054, India*

^l*Experimental Animal Facility, Institute of Nuclear Medicine and Allied Sciences, Defence Research and Development Organization, Brig. S.K. Mazumdar Marg, New Delhi-110054, India*

^d*Department of Chemistry, SVGC Ghumarwin, Bilaspur, Himachal Pradesh-174021, India*

*Corresponding authors: rashimathur07@gmail.com: akmishra63@gmail.com (Rashi Mathur and Anil Kumar Mishra)

REFERENCES

- (1) I. L. Medintz, H.T. Uyeda, E. R. Goldman and H. Mattoussi, *Physica E Low Dimens. Syst. Nanostruct.*,2004, **25**(1), 1-12.
- (2) J. K. Jaiswal, H. Mattoussi, J. M. Mauro and S. M. Simon,*Nat. Biotechnol.*2003, **21**, 47-51.

- (3) B. Ballou, B. Lagerholm, L. Ernst, M. Bruchez and A. Waggoner, *Bioconjugate Chem.*, 2004, **15**, 79-86.
- (4) R. E. Bailey, A. M. Smith and S. Nie, *Physica E Low Dimens. Syst. Nanostruct.*, 2004, **25**, 1-12.
- (5) M. Bruchez, M. Moronne, P. Gin, S. Weiss and A. P. Alivisatos, *Science*, 1998, **281**, 2013-2016.
- (6) P. Suriamoorthy, X. Zhang, G. Hao, A. G. Joly, S. Singh, M. Hossu, X. Sun and W. Chen, *Cancer Nanotech.*, 2010, **1**, 19-28.
- (7) X. Gao, Y. Cui, R. M. Levenson, L. W. K. Chung and S. Nie, *Nat. Biotechnol.*, 2004, **22**, 969-976.
- (8) U. R. Genger, M. Grabolle, S. C. Jaricot, R. Nitschek and T. Nann, *Nat. Methods.*, 2008, **5**, 763-775.
- (9) Y. Su, M. Hu, C. Fan, Y. He, Q. Li, W. Li, L. Wang, P. Shen and Q. Huang, *Biomaterials*, 2010, **31**, 4829-4834.
- (10) N. Chen, Y. He, Y. Su, X. Li, Q. Huang, H. Wang, X. Zhang, R. Tai and C. Fan, *Biomaterials*, 2012, **33**, 1238-1244.
- (11) X. Wu, F. Tian, J. X. Zhao and M. Wu, *Expert. Opin. Drug. Metab. Toxicol.*, 2013, **9**(10), 1165-1277.
- (12) H. C. Fischer and C. W. C. Chan, *Curr. Opin. Biotech.*, 2007, **18**, 565-571.
- (13) A. Nei, T. Xia, L. Maedler and N. Li, *Science*, 2006, **311**, 622-627.
- (14) A. M. Derfuse, C. W. C. Chan and S. N. Bhatia, *Nano Lett.*, 2004, **4**, 11-18.
- (15) C. Kirchner, T. Liedl and S. Kudara, *Nano Lett.*, 2005, **5**, 331-338.
- (16) J. Lorvic, J. S. Cho, F. M. Winnik and D. Maysinger, *Chem. Biol.*, 2005, **12**, 1227-1234.
- (17) S. J. Cho, D. Maysinger, M. Jain, B. Roder, S. Hackberth and F. M. Winnik, *Langmuir*, 2007, **23**, 1974-1980.
- (18) B. Dubertret, P. Skourides, D. J. Norris, V. Noireaux, A. H. Brivanlou and A. Libchaber, *Nat. Mater.*, 2005, **4**, 435-446.
- (19) W. C. W. Chan, D. J. Maxwell, X. Gao, R. E. Bailey, M. Han and S. Nie, *Curr. Opin. Biotech.*, 2002, **13**, 40-46.
- (20) S. J. Tan, N. R. Jana, S. Gao, P. K. Patra and J. Y. Ying, *Chem. Mater.*, 2010, **22**, 2239-2247.
- (21) K. Pathakoti, H. M. Hwang, H. Xu, Z. P. Aguilar and A. Wang, *J. Environ. Sci.*, 2013, **25**, 163-171.
- (22) K. M. Tsoi, Q. Dai, B. A. Alman and C. W. C. Chan, *Acc. Chem. Res.*, 2013, **19**, 662-671.
- (23) S. H. Tanya, E. A. Robin, C. F. Hans, N. Susan and C. W. C. Warren, *Small*, 2009, **6**, 138-144.
- (24) R. H. Yang, L. W. Chang and J. P. Wu, *Environ. Health Perspect.*, 2007, **115** (9), 1339-1343.
- (25) Y. Su, F. Peng, Z. Jiang, Y. Zhong, Y. Lu, X. Jiang, Q. Huang, C. Fan, S. Lee and Y. He, *Biomaterials*, 2011, **32**, 5855-5862.
- (26) A. Galeone, G. Vecchio, M. A. Malvindi, V. Brunetti, A. Cingolani and P. P. Pompa, Genotoxicity. *Nanoscale*, 2012, **4**, 6401-6407.
- (27) H. Fischer, L. Liu, K. Pang and C. W. C. Chan, *Adv. Funct. Mater.*, 2006, **16**, 1299-1305.
- (28) D. K. Tiwari, T. Jin and J. Behari, *Int. J. Nanomed.*, 2011, **6**, 463-475.
- (29) A. Hashino, K. Fujioka and T. Oku, *Nano Lett.*, 2004, **4**, 2163-2169.
- (30) L. Peng, M. He, B. Chen, Q. Wu, Z. Zhang, D. Pang, Y. Zhu and B. Hu, *Biomaterials*, 2013, **34**, 9545-9558.
- (31) Y. Tang, S. Han, H. Liu, X. Chen, L. Huang, X. Li and J. Zhang, *Biomaterials*, 2013, **34**, 8741, 87-55.
- (32) M. L. Schipper, G. Iyer, A. L. Koh, Z. Cheng, Y. Ebenstein, A. Aharoni, S. Keren, L. A. Bentolila, J. Li, J. Rao, U. Banin, A. M. Wu, R. Sinclair, S. Weiss and S. S. Gambhir, *Small*, 2009, **5**, 126-134.
- (33) N. Bag, R. Mathur, S. Singh, F. Hussain, R. P. Chauhan, K. Chuttani, and A. K. Mishra, *Med. Chem. Commun.*, 2015, **2** (6), 363-371
- (34) A. R. Fritzbler, P. G. Abrams, P. L. Beaumier, S. Kasina, A. C. Morgan, T. N. Rao, J. M. Reno, J. A. Sanderson, A. Srinivasan, D. A. Wilbur and J. Vanderheyden, *Proc. Natl. Acad. Sci.*, 1988, **85**, 4025-4029.
- (35) M. M. Bisunandan, P. J. Blower, S. E. M. Clarke, J. Singh, M. J. West., *Appl. Radiat. Isot.* 1991, **42**, 167-171
- (36) E. Dadachova, J. Chapman, 1998, *Nucl. Med. Commun.*, **19**, 173-181
- (37) I. F. F. Benzie and J. Strain, *Anal. Biochem.*, 1996, **239**, 70-76.
- (38) V. Katalinic, D. Modun, I. Music and M. Boban, *Comp. Biochem. Physiol., Part C: Toxicol. Pharmacol.*, 2005, **140** (1), 47-52.
- (39) S. H. Choi, W. Liu and P. Misra, *Nat. Biotechnol.*, 2007, **25**, 1165-1170.
- (40) H. C. Fischer, T. S. Hauack, A. G. Aristizabal and W. C. W. Chan, *Adv. Mater.*, 2010, **22**, 2520-2524.
- (41) K. G. Li, J. T. Chen, S. S. Bai, X. Wen, S. Y. Song, Q. Yu, J. Li and Y. Q. Wang, *Toxicol. In Vitro*, 2009, **23**, 1007-1013.
- (42) K. C. Nguyen, W. G. Willmore and A. F. Tayabali, *Toxicology*, 2013, **306**, 114-123.

Table 2 Alteration in hematological parameters in control and treated rats
1,3,7,10,15 days of post injection

Parameters (units)	Control	Day 1	Day 3	Day 7	Day 10	Day15
WBC($10^3/\mu\text{l}$)	13.5 \pm .02	6.8 \pm 0.03	10.6 \pm .01	9.6 \pm .01	15.4 \pm 0.02	15.5 \pm 0.05
RBC($10^{12}/\mu\text{l}$)	8.01 \pm .06	7.83 \pm .06	7.73 \pm .03	7.48 \pm .08	7.86 \pm .03	7.31 \pm 0.02
HGB (g/dl)	15.0 \pm .18	15.1 \pm .18	14.6 \pm .12	14.9 \pm .11	14.9 \pm .11	14.5 \pm 0.15
HCT(%)	41.05 \pm 1.2	41.4 \pm 2.1	40.8 \pm 1.8	40.8 \pm 2.1	40.8 \pm 2.1	39.5 \pm 2.2
MCV (fl)	52.9 \pm 2.2	52.7 \pm 1.9	53.6 \pm 2.8	53.3 \pm 2.6	53.3 \pm 2.6	53.9 \pm 2.7
MCHC (g/dl)	56.4 \pm 2.1	36.5 \pm 3.1	35.9 \pm 2.6	36.3 \pm 3.1	36.3 \pm 3.1	36.0 \pm 3.4
PLT($10^3/\mu\text{l}$)	1011 \pm 19.7	1028 \pm 32.3	1018 \pm 21.9	1149 \pm 34.2	1149 \pm 34.2	1188 \pm 29.5
LY(%)	69.5 \pm 3.1	67.6 \pm 4.5	68.3 \pm 3.2	70.3 \pm 2.7	70.3 \pm 2.7	62.6 \pm 3.2
GR(%)	30.5 \pm 1.7	34.4 \pm 4.3	31.1 \pm 3.0	29.6 \pm .8	29.6 \pm 2.8	37.5 \pm 2.6
RDW(%)	11.2 \pm .09	11.6 \pm .07	10.9 \pm 0.05	11.4 \pm .08	11.4 \pm .08	11.5 \pm 0.03
PCT(%)	0.51 \pm .01	0.47 \pm .09	0.43 \pm 0.03	0.52 \pm .01	0.52 \pm .01	0.52 \pm .01
MPV (fl)	4.2 \pm .09	4.3 \pm .09	4.1 \pm .01	4.2 \pm .03	4.2 \pm .03	4.5 \pm 0.06

Values are in: Mean \pm standard deviation

WBC- white blood cells, RBC-red blood cells,HGB- haemoglobin,HCT- hematocrit, MCV- mean corpuscular volume, MCHC- mean corpuscular haemoglobin concentration, PLT- platelets, LY- lymphocytes, GR- granulocytes, RDW- red cell distribution width, PCT- plateletcrit, MPV- mean platelet volume.